

	SAKARYA UNIVERSITY JOURNAL OF SCIENCE				 <b>SAKARYA</b> UNIVERSITY
	e-ISSN: 2147-835X <a href="http://www.saujs.sakarya.edu.tr">http://www.saujs.sakarya.edu.tr</a>				
	Received	Revised	Accepted	DOI	
06.05.2018	03.07.2018	31.05.2018	10.16984/saufenbilder.421351		

## System Constrained Active Power Loss Minimization in Practical Multi-terminal HVDC Systems through GA

Faruk Yalçın<sup>\*1</sup>, Uğur Arifoğlu<sup>2</sup>

### Abstract

In this paper, a novel optimal reactive power flow solution approach in multi-terminal HVDC (High Voltage Direct Current) systems is studied. ULTCs' (under load tap changer transformers) full equivalent model for the DC converters' are taken into account in the proposed AC-DC power unlike the similar studies in the literature. Thus, the proposed study provides real accurate results for practical AC-DC applications. Optimal reactive power flow for minimum active power loss is provided by Genetic Algorithm (GA). For the test of the proposed study, the IEEE 14-bus test system modified to AC-DC system is used in the study. The obtained test results prove that the proposed GA based optimization method is effective to reach the global optimum point of minimum active power loss without dropping to local minimum point through satisfying system constraints.

**Keywords:** active power loss minimization, HVDC, multi-terminal, ULTC, genetic algorithm

### 1. INTRODUCTION

Reactive power flow in power transmission lines is one of the important issue in power systems. The transmission lines are lossy as they have resistive characteristic. So, some part of the generated active power by the generators is lost on the lines. This situation causes economic loss. On the other hand, it requires to allocate new transmission lines to meet the increasing power demand. Allocation of new transmission lines is both non-economic and very difficult. So, minimization of active power loss is so important. As active power loss is dependent on the reactive power flowing through

the transmission lines, this is achieved by optimal reactive power flow [1].

The built-up costs of HVDC systems are too expensive. But they can be economic than traditional AC lines for longer distances. On the other hand, system reliability and consistency, efficient establishment, efficient conductor intersection, etc. are the advantages of the DC systems [2]. Because of these mentioned advantages and reasons, there are many studies on integrated DC systems into traditional AC systems in the literature. Many techniques are proposed for the integrated AC-DC power flow studies based on simultaneous technique and sequential technique.

\* Corresponding Author

<sup>1</sup>Department of Mechatronics Engineering, Faculty of Technology, Sakarya University, Sakarya, TURKEY, farukyalcin@sakarya.edu.tr

<sup>2</sup>Department of Electrical-Electronics Engineering, Faculty of Engineering, Sakarya University, Sakarya, TURKEY, arifoglu@sakarya.edu.tr

In the sequential technique, AC and DC power flows are executed separately [3]. In simultaneous technique, all equations of the AC-DC system are together and solution of them in the same algorithm [4].

The studies for AC-DC optimal power flow in the literature are not sufficient even though there are many researches for traditional power flow of AC-DC systems. AC-DC optimal power flow studies in the literature are implemented successfully by using well-known numerical optimization methods [5-12]. But on the other hand, they have convergence and dropping to local minimum point problems [13].

The new trend heuristic methods like the artificial bee colony algorithm [14], the differential evolution algorithm [15], the particle swarm optimization algorithm [16] and the artificial ant colony algorithm [17] are increasingly used for the global optimization problem solutions and they are applied to different kind of optimization problems successfully. These methods are more effective for not dropping to local minimum point, faster convergence and providing better optimized solution than the traditional numerical techniques as mentioned before.

GA (genetic algorithm) is a kind of the heuristic techniques mentioned above and it is efficiently used for optimal power flow applications in traditional AC power systems as well as in many different kind optimization solutions in many different areas [18-19].

In the presented paper, a new approach has been presented for the minization of active power loss in multi-terminal HVDC systems using GA. The sequential technique is used for active power loss minimization of the AC-DC system and full equivalent model of ULTCs in the both DC and AC systems are considered in the AC-DC power flow algorithm to be used in practical applications. GA is used for the optimization of optimal reactive power flow to minimize the total active power loss. On the other hand, the full system constraints of the both the control variables and the state variables are also taken into account in the optimal reactive power flow. The presented approach is applied to the modified IEEE 14-bus AC-DC test system to test the accuracy and the efficiency of the presented approach.

## 2. THE PROPOSED SEQUENTIAL AC-DC POWER FLOW ALGORITHM

This section presents the proposed AC-DC power flow algorithm. As mention before, sequential method is chosen for AC-DC power flow. So, the subsections demonstrate the sequential AC and the sequential DC power flow algorithms.

### 2.1. The Proposed Sequential AC Power Flow Algorithm

In this subsection, the proposed sequential AC power flow algorithm that is used in this active power loss minimization of integrated HVDC system is presented. The well known Newton-Raphson method is chosen to solve the AC power flow problem. The full equivalent model of the ULTCs' of the DC converters' are taken into account like the ULTCs connected to AC buses in this study. The ULTC's model and its equivalent circuit are represented in Fig. 1 [20].

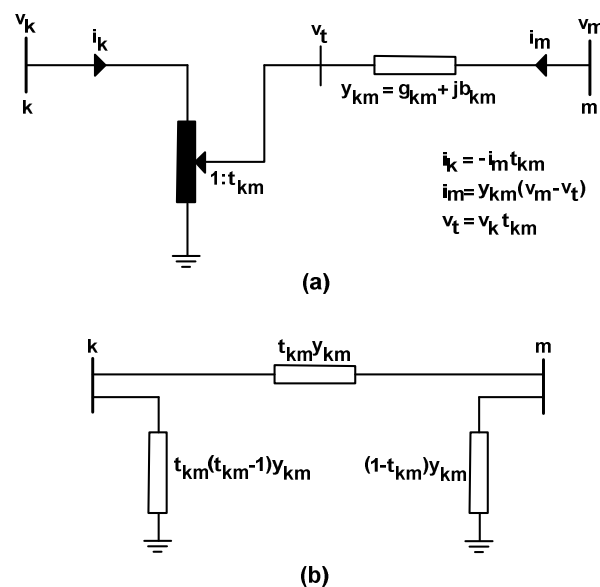


Figure 1. Model of ULTC a) general circuit of ULTC b) equivalent circuit of ULTC

in Fig. 1;  $k$  ,  $m$  ,  $t_{km}$  and  $y_{km}$  determine the ULTC's primary side bus, the secondary side bus, the ULTC's tap value and winding admittance values of the ULTCs, respectively.

$$y_{km} = g_{km} + jb_{km} \tag{1}$$

The series and shunt admittance values in Fig. 1 change in the sequential DC power flow as the tap

values of the ULTCs connected to the DC converters are force to change. Because of this, the AC system bus admittance matrix has to be reorganised for the updated tap values of the ULTCs. In the proposed approach, just  $y_{km}$ , the admittance value of the ULTC's serial winding is taken into account in  $y_{bus}$  AC bus admittance matrix. The values of the shunt admittances of bus  $k$  and bus  $m$  are accepted as zero for preventing reorganising of  $y_{bus}$ . Depending on these conditions,  $p_k$ ,  $q_k$ ,  $p_m$  and  $q_m$  which are the active powers and the reactive powers injected from the subscript buses to other ones in AC network can be formulated as;

$$p_k = v_k \sum_{\substack{j=1 \\ j \neq k, m}}^{nb} v_j \left( g_{bus_{kj}} \cos \delta_{kj} + b_{bus_{kj}} \sin \delta_{kj} \right) + v_k v_m t_{km} \left( g_{bus_{km}} \cos \delta_{km} + b_{bus_{km}} \sin \delta_{km} \right) + v_k^2 \left[ g_{bus_{kk}} - (t_{km}^2 - 1) g_{bus_{km}} \right] \quad (2)$$

$$q_k = v_k \sum_{\substack{j=1 \\ j \neq k, m}}^{nb} v_j \left( g_{bus_{kj}} \sin \delta_{kj} - b_{bus_{kj}} \cos \delta_{kj} \right) + v_k v_m t_{km} \left( g_{bus_{km}} \sin \delta_{km} - b_{bus_{km}} \cos \delta_{km} \right) + v_k^2 \left[ -b_{bus_{kk}} + (t_{km}^2 - 1) b_{bus_{km}} \right] \quad (3)$$

$$p_m = v_m \sum_{\substack{j=1 \\ j \neq m, k}}^{nb} v_j \left( g_{bus_{mj}} \cos \delta_{mj} + b_{bus_{mj}} \sin \delta_{mj} \right) + v_m v_k t_{km} \left( g_{bus_{mk}} \cos \delta_{mk} + b_{bus_{mk}} \sin \delta_{mk} \right) + v_m^2 g_{bus_{mm}} \quad (4)$$

$$q_m = v_m \sum_{\substack{j=1 \\ j \neq m, k}}^{nb} v_j \left( g_{bus_{mj}} \sin \delta_{mj} - b_{bus_{mj}} \cos \delta_{mj} \right) + v_m v_k t_{km} \left( g_{bus_{mk}} \sin \delta_{mk} - b_{bus_{mk}} \cos \delta_{mk} \right) - v_m^2 b_{bus_{mm}} \quad (5)$$

Here,  $n_b$  represents the bus number,  $v_i$  represents the bus voltage value,  $g_{bus_{ij}}$  represents the conductance value of the bus admittance matrix

related component,  $b_{bus_{ij}}$  represents the susceptance value of the bus admittance matrix related component,  $b_{bus_{ij}}$  and  $\delta_{ij}$  represents the phase angle difference between the related bus voltages.

The powers injected from the buses different than the buses  $k$  and  $m$  are defined as,

$$p_i = v_i \sum_{j=1}^{nb} v_j \left( g_{bus_{ij}} \cos \delta_{ij} + b_{bus_{ij}} \sin \delta_{ij} \right) \quad (6)$$

$$q_i = v_i \sum_{j=1}^{nb} v_j \left( g_{bus_{ij}} \sin \delta_{ij} - b_{bus_{ij}} \cos \delta_{ij} \right) \quad (7)$$

The demonstration for the general bus of the integrated HVDC system used in this optimal reactive power flow study is given in Fig. 2. In Fig. 2,  $p_{gi}$ ,  $q_{gi}$ ,  $p_{di}$ ,  $q_{di}$ ,  $p_{li}$ ,  $q_{li}$ ,  $q_{ci}$ ,  $p_i$  and  $q_i$  represent the related bus' generator active power, the related bus' generator reactive power, the related DC converter's active power, the related DC converter's reactive power, the related bus' load active power, the related bus' load reactive power, the shunt reactive power supply reactive power, the active power flowing from the related bus to the other ones in AC system defined in (2), (4), (6) and the reactive power flowing from the related bus to the other ones in AC system defined in (3), (5), (7), respectively.

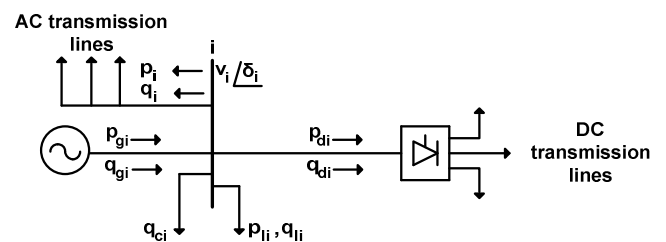


Figure 2. General bus demonstration of the proposed integrated HVDC system

The DC converters's active and reactive powers have been accepted as constant loads in the AC buses where no DC converters exist in the presented AC power flow algorithm. The values of the active powers and the reactive powers of the converters are updated at the end of the DC algorithm that is explained in the next subsection. And they are sent to the AC power flow algorithm when the sequential DC power flow algorithm

converges. Thus, the equations that must be provided in the Newton-Raphson based power flow algorithm for general bus demonstration given in Fig. 2 are given as,

$$g_{pi} = p_i + p_{d_i} + p_{l_i} - p_{g_i} = 0 \quad (i = 2, \dots, n_b) \quad (8)$$

$$g_{qi} = q_i + q_{d_i} + q_{l_i} - q_{c_i} = 0 \quad (i = n_g + 1, \dots, n_b) \quad (9)$$

where  $n_g$  represents the total generator bus number in the system.

The ULTCs' tap values that are connected to the DC converters are changed in the sequential DC power flow algorithm as mentioned before and they are taken into account as constant control variables during the AC power flow study. So, the control variables and the state variables for the presented AC power flow can be defined as,

$$x_{AC} = [\delta_2, \dots, \delta_{n_b}, v_{ng+1}, \dots, v_{n_b}] \quad (10)$$

$$u_{AC} = [p_{g2}, \dots, p_{gng}, v_1, \dots, v_{ng}, t_1 \dots t_{nt}, t_{d_1} \dots t_{d_{nd}}] \quad (11)$$

Here,  $t$  represents the ULTC tap value where the ULTC is not connected to any converter,  $n_t$  represents the total ULTCs number where the ULTC is not connected to any converter,  $t_d$  represents the ULTC tap value where the ULTC is connected to a converter and  $n_{td}$  represents the total ULTC number where they are connected to a converter, respectively.

### 2.2. The Proposed Sequential DC Power Flow Algorithm

The subsection demonstrates the proposed sequential DC power flow algorithm based on the proposed DC power model shown in Fig. 3.

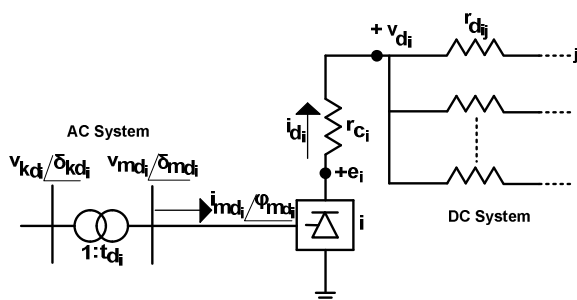


Figure 3. The presented DC power model of multi-terminal integrated AC-DC system

Here in Fig. 3,  $e_i$  represents the open circuit direct voltage of the converter,  $v_{d_i}$  represents the terminal direct voltage of the converter,  $i_{d_i}$  represents the direct current of the converter,  $r_{c_i}$  represents the commutation resistance of the converter,  $r_{d_{ij}}$  represents the DC line resistance between the related converters,  $t_{d_i}$  represents the ULTC tap value of the related converter,  $v_{kd_i}$  represents the ULTC primary side alternative voltage at the related converter station,  $v_{md_i}$  represents the ULTC primary side alternative voltage at the related converter station,  $i_{md_i}$  represents the value of the alternative current flowing from the ULTC secondary side to the converter,  $\delta_{kd_i}$  represents the phase angle of the ULTC primary side alternative voltage at the related converter station,  $\delta_{md_i}$  represents the phase angle of the ULTC secondary side alternative voltage at the related converter station and  $\varphi_{md_i}$  represents the alternative current flowing from the ULTC secondary side to the converter at the related converter station, respectively.

The open circuit direct voltages of the converters can be given as,

$$e_i = v_{md_i} \cos \theta_i \quad (i = 1, \dots, n_c) \quad (12)$$

Here,  $n_c$  represents the total converter number in the DC system.  $\theta_i$  defines  $\alpha_{d_i}$  and  $\gamma_{d_i}$  and it is either the firing angle or extinction/recovery angle of the converter where the converter operates in the rectifier mode or the inverter mode, respectively.

The converters' terminal direct voltages are given as,

$$v_{d_i} = e_i - r_{c_i} i_{d_i} \quad (i = 1, \dots, n_c) \quad (13)$$

The commutation resistance  $r_{c_i}$  is positive if the converter operates in the rectifier mode or it is negative if the converter operates in the inverter mode in (13).

The phase demonstrated in Fig. 3 can be formulated as,

$$\phi_{md_i} = \delta_{md_i} - \varphi_{md_i} \quad (i = 1, \dots, n_c) \quad (14)$$

and it is also obtained as,

$$\phi_{md_i} = \arccos\left(\frac{v_{d_i}}{v_{md_i}}\right) \quad (i = 1, \dots, n_c) \quad (15)$$

The active powers and the reactive powers of the converters are formulated as,

$$p_{d_i} = v_{d_i} i_{d_i} \quad (i = 1, \dots, n_c) \quad (16)$$

$$q_{d_i} = |p_{d_i} \tan \phi_{md_i}| \quad (i = 1, \dots, n_c) \quad (17)$$

The multi-terminal DC system model can be represented as in Fig. 4. The sign of the commutation resistance values change in each iteration if the converter operation modes are changed from the inverter mode to the rectifier mode or vice versa. Because of this situation, in the presented DC power flow study, the commutation resistances are excluded from the DC bus resistance matrix to prevent reorganising of the bus resistance matrix in every DC algorithm iteration by the given model. If the  $v_{d_i}$  values of the converters are accepted as source voltages in the calculations, the commutation resistance values can be excluded from the DC bus resistance matrix and it is given as,

$$r_{d_{bus}} = y_{d_{bus}}^{-1} \quad (18)$$

where  $y_{d_{bus}}$  represents the DC bus admittance matrix and it has just the admittance values of the DC transmission lines.

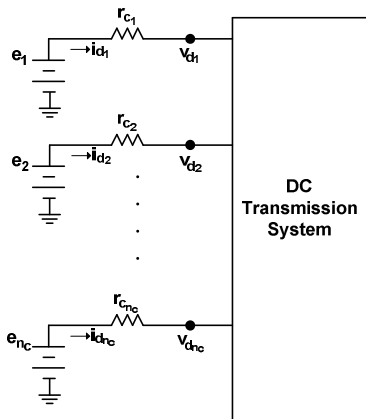


Figure 4. The multi-terminal DC system model

By considering the terminal voltage of the first converter as reference voltage value, the values of the open circuit direct voltages of the converters can be given as,

$$e_1 = v_{d_1} + r_{c_1} i_{d_1} \quad (19)$$

$$e_i = e_1 - r_{c_1} i_{d_1} + r_{c_i} i_{d_i} + \sum_{j=2}^{n_c} r_{d_{bus,j}} i_{d_j} \quad (i = 2, \dots, n_c) \quad (20)$$

Depending to the multi-terminal model shown in Fig. 4, the algebraic summation value of the s direct currents values of the converters has to be zero according to Kirchhoff voltage law,

$$\sum_{i=1}^{n_c} i_{d_i} = 0 \quad (21)$$

In the presented study, the active power values of all converters except one of them are chosen as the control variables for optimal reactive power flow of active power loss minimization in the presented paper. This consideration is accepted for achieving the best suitable active powers for the converters and the best suitable converter operation modes which enhance the minimization of the total active power loss.

### 2.3. The Demonstration of the Proposed Sequential AC-DC Power Flow Algorithm

The obtained sequential AC-DC power flow algorithm from the presented sequential AC and DC power flow algorithms demonstrated in the subsections 2.1 and 2.2 is explained through a flowchart in this subsection. The presented AC-DC power flow algorithm is shown in detailed in Fig. 5.

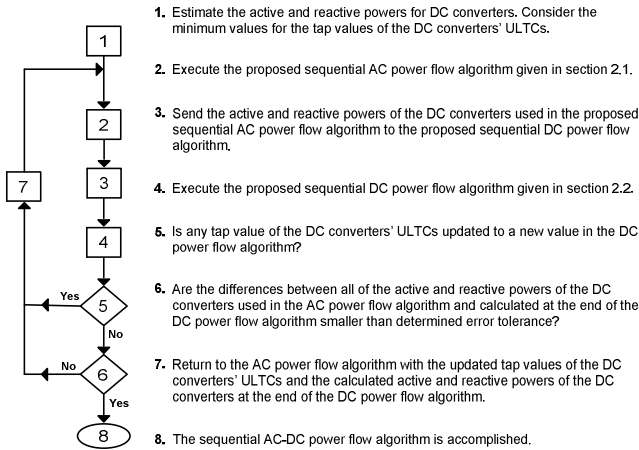


Figure 5. The proposed AC-DC power flow algorithm

### 3. THE OPTIMAL ACTIVE POWER LOSS MINIMIZATION PROBLEM

Below, the optimization formula for the optimal reactive power flow to minimize active power loss in integrated HVDC system can be given as,

$$\begin{aligned} & \text{Minimize} && f(x,u) \\ & \text{Subjected to} && g(x,u) \ \& \ h(x,u) \end{aligned} \tag{22}$$

Here  $f(x,u)$  represents the objective function,  $g(x,u)$  represents the equality constraints,  $h(x,u)$  represents the inequality constraints,  $x$  represents the state variables and  $u$  represents the control variables, respectively.

AC-DC system total active power loss in the proposed is formulated as below:

$$P_{loss} = \sum_{i=1}^{n_g} P_{gi} - \sum_{i=1}^{n_b} P_{li} - \sum_{i=1}^{n_c} P_{di} \tag{23}$$

The equality constraints for the AC system,

$$P_{gi} - P_{li} - P_{di} - P_i = 0 \tag{24}$$

$$Q_{gi} + Q_{sci} - Q_{li} - Q_{di} - Q_i = 0 \tag{25}$$

where  $Q_{sci}$  represents the reactive power of the synchronous condensers.

The equality constraints for the DC system,

$$\sum_{i=1}^{n_c} I_{di} = 0 \tag{26}$$

The equality constraints in (24-26) represented as  $g(x,u)$  are provided in the proposed AC-DC power flow algorithm explained in previous section.

The AC system inequality constraints can be given as,

$$P_{gi}^{\min} \leq P_{gi} \leq P_{gi}^{\max} \tag{27}$$

$$Q_{gi}^{\min} \leq Q_{gi} \leq Q_{gi}^{\max} \tag{28}$$

$$Q_{sci}^{\min} \leq Q_{sci} \leq Q_{sci}^{\max} \tag{29}$$

$$V_i^{\min} \leq V_i \leq V_i^{\max} \tag{30}$$

$$t_i^{\min} \leq t_i \leq t_i^{\max} \tag{31}$$

where  $t_i$  represents the tap values of the ULTCs connected AC buses where any DC converters are not connected to, min and max superscripts represent the lower and upper limits of the associated variables, respectively.

The DC system inequality constraints can be given as,

$$P_{di}^{\min} \leq P_{di} \leq P_{di}^{\max} \tag{32}$$

$$V_{di}^{\min} \leq V_{di} \leq V_{di}^{\max} \tag{33}$$

$$t_{di}^{\min} \leq t_{di} \leq t_{di}^{\max} \tag{34}$$

The proposed DC power flow algorithm automatically provides the inequality given in (34).

The state variables for whole AC-DC system are given as,

$$x = [x_{AC}, x_{DC}] \tag{35}$$

where  $x_{AC}$  and  $x_{DC}$  represent the state variables of the AC and the DC system, respectively.

$$x_{AC} = [\delta_2, \dots, \delta_{nb}, v_1, \dots, v_{nl}] \tag{36}$$

$$x_{DC} = [I_{d1}, \dots, I_{dnc}, V_{d1}, \dots, V_{dnc}] \tag{37}$$

Here  $\delta_i$  represents the AC bus voltage angle and  $n_l$  represents the load bus number of AC system where no synchronous condenser connects to, respectively.

The control variables for the whole AC-DC system can be given as,

$$u = [u_{AC}, u_{DC}] \quad (38)$$

Here  $u_{AC}$  represents the control variables of the AC system and  $u_{DC}$  represents the control variables of the DC system, respectively.

$$u_{AC} = [p_{g2}, \dots, p_{gng}, v_1, \dots, v_{ng}, v_1, \dots, v_{nsc}, t_1, \dots, t_{nt}] \quad (39)$$

$$u_{DC} = [p_{d2}, \dots, p_{dnc}] \quad (40)$$

Here  $n_i$  represents the total number of the ULTCs that connect to AC buses and  $n_{sc}$  represents the total number of the synchronous condensers used in AC system, respectively. It must be noted that there is a difference between (11) and (39), the existing of  $t_{di}$  values in (11). As mentioned in section 2.1, in fact,  $t_{di}$  values are not part of the AC systems, but they are presented in (11) to show that they are considered in the sequential AC power flow algorithm as control values.

The optimal reactive power flow in the multi-terminal HVDC system aims to optimize the total active power loss to be minimized given by (23) through providing the system constraints defined in (27-33) represented as  $h(x, u)$ . So, the objective function which must be optimized is given below,

$$\begin{aligned} f(x, u) = & c_1 \cdot p_{loss} + c_2 \cdot \sum_{i=1}^{n_g} |p_{gi} - p_{gi}^{lim}| \\ & + c_3 \cdot \sum_{i=1}^{n_g} |q_{gi} - q_{gi}^{lim}| + c_4 \cdot \sum_{i=1}^{n_{sc}} |q_{sci} - q_{sci}^{lim}| \\ & + c_5 \cdot \sum_{i=1}^{n_b} |v_i - v_i^{lim}| + c_6 \cdot \sum_{i=1}^{n_t} |t_i - t_i^{lim}| \\ & + c_7 \cdot \sum_{i=1}^{n_c} |p_{di} - p_{di}^{lim}| + c_8 \cdot \sum_{i=1}^{n_c} |v_{di} - v_{di}^{lim}| \end{aligned} \quad (41)$$

Here  $c_i$  defines the the objective function's penalty coefficient values. The variables that includes lim superscript is given below,

$$(x, u)^{lim} = \begin{cases} (x, u), (x, u)_{min} \leq (x, u) \leq (x, u)_{max} \\ (x, u)_{min}, (x, u) < (x, u)_{min} \\ (x, u)_{max}, (x, u) > (x, u)_{max} \end{cases} \quad (42)$$

#### 4. GA AND ITS APPLICATION FOR OPTIMAL REACTIVE POWER FLOW PROBLEM

GA is one of the heuristic optimization techniques which is based on evolutionary process and it is firstly presented for the general optimization applications by Holland in 1975. GA is based on natural selection. The details of the GA can be found in [21].

The proposed flow chart for the active power loss minimization of the optimal reactive power flow in the presented practical multi-terminal HVDC system through GA can be detailed in Fig. 6. The main stages of GA based on natural selection can be defined in 3 stages. These stages are “human is born”, “human grows” and “human dies”. The optimization algorithm parameters that are used for producing the objective function which is optimized through the genetic algorithm can be represented by the gens in GA. For the optimal reactive power flow solution, the parameters represented as gens define the control variables given by (38). The gens set is considered as an individual in GA. According to the natural selection process, the individual defines human in GA. The all individuals used in GA produce the population. Main stages of GA optimization technique is given as follows; the initial population stage, the fitness scaling stage, the selection stage, the crossover stage, the mutation stage and the optimization criterion stage [22].

In the initial population stage, the initial population GA is produced and it can be defined as,

$$w_{ij} = w_{min,j} + rand(0,1) \times (w_{max,j} - w_{min,j}) \quad (43)$$

$$(i = 1 \dots n_{ind}) \quad (j = 1 \dots n_p)$$

Here  $n_{ind}$  represents the total number of the individuals exist in the population,  $n_p$  represents the total number of the parameters (gens) belong to the individuals,  $w_{min,j}$  represents the parameters minimum values and  $w_{max,j}$  represents the parameters maximum values, respectively.

The individuals are defined in the fitness scaling stage to be used in the selection stage.

$$fit_{ave} = \frac{\sum_{i=1}^{n_{ind}} fit_i}{n_{ind}} \quad (44)$$

Here  $fit_{ave}$  represents the population average fitness value and  $fit_i$  represents related individual's fitness value, respectively.  $fit_i$  defines the objective function given by (41). The individuals that have better, in other words smaller fitness values than the average fitness value are transferred to the selection stage to be used there.

In the selection stage, the parents are selected from the determined individuals and they are crossed to produce children. To select the parents from the defined individuals for producing the children, the tournament method is used. The tournament method formulation is given as,

$$g_i = \frac{fit_i}{\sum_{j=1}^{n_{ind}} fit_j} \quad (45)$$

Here,  $g_i$  represents the individual's weight. The individual's weight determines the probability of the election in this selection stage. Here, the sum of the individuals' weights in the population must equal to 1.

$$\sum_{i=1}^{n_{ind}} g_i = 1 \quad (46)$$

The children number is determined at the beginning of the algorithm. The number of the individuals which will be selected from the population and be used for parent selection is determined as twice of the children number. The parents with the same children number are selected from these selected individuals.

The children are produced by parents determined by the selection stage in the crossover stage and these children are considered as new individuals. The new children individuals in the same children number are produced by using the crossing technique. 1 and 0 values in the same individual's gen number are produced randomly for crossing process. If the randomly produced value is determined as 0, then this means that the gen is taken from father. If the randomly produced value is determined as 1, then this means that the gen is

taken from mother. Thus, the child is produced by crossing. Crossing process can be exemplified as below:

Cross: 1 0 0 1 0

Father: u w x y z

Mother: a b c d e

Child: a w x d z

In the mutation stage, some new individuals are created to change some or all of the gens of the selected individuals. These selected individuals are forced to be mutated. The number of the individuals that are mutated is determined at the beginning of GA. These individuals are recreated to be formed all the gens of the selected individuals within the algorithm. So, new individuals with the same selected individuals number which are mutated are produced randomly through (43). Mutation process increases the variety of the population. Thus, it provides obtaining better solutions through preventing losing the good individuals.

There are many kind of stopping criteria for optimization which is executed by GA and the similar heuristic techniques in the literature. In this paper, iteration number is chosen for stopping criterion of the studied optimization through GA. The stopping iteration number is selected as 100 for the study. GA stops when the algorithm reaches the determined iteration number, 100. On the other hand, in this study, system constraints defined (27-33) are included in the optimization stopping criterion so that all of the system constraints are provided at the end of GA.

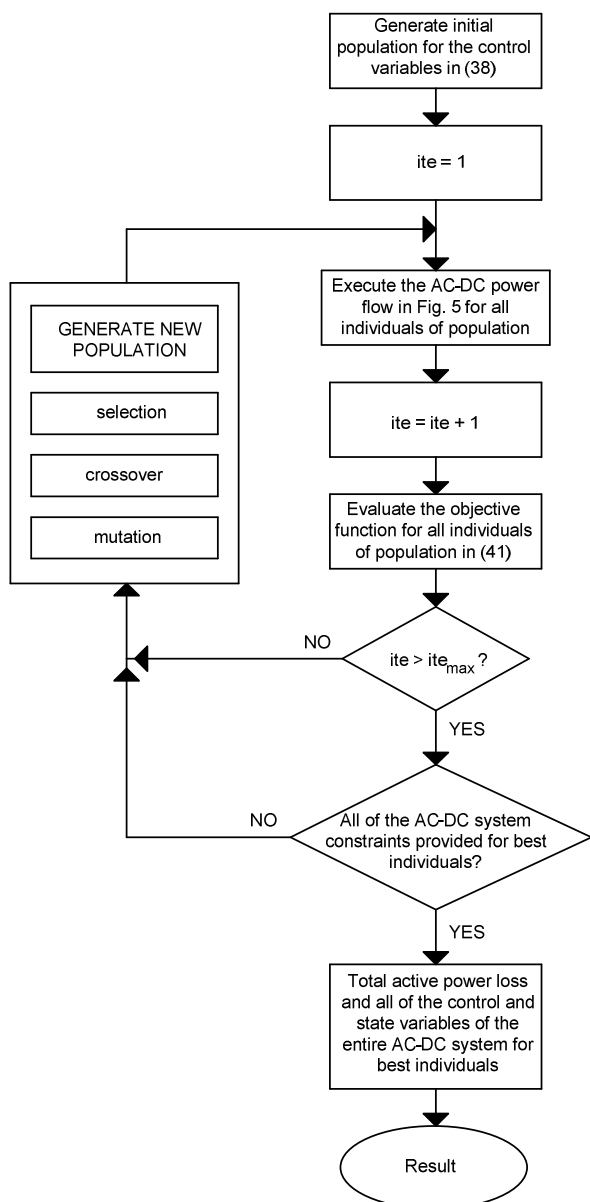


Figure 6. The proposed flow chart for active power loss minimization in multi-terminal HVDC system by GA

### 5. RESULTS

The efficiency and the accuracy of the presented approach are tested on the modified IEEE 14-bus AC-DC test system given by Fig. 7.

Total active power loss throughout the proposed GA based optimization algorithm is demonstrated graphically in Fig. 8. Total active power loss obtained with proposed GA based approach and another traditional numerical method, steepest descent algorithm (SDA), are compared in the same test system. In the literature, generally, 100 iterations are performed for heuristic methods. So,

100 iterations application is chosen for the proposed GA for the optimization. The proposed optimization algorithm is performed for 50 optimization trials with different AC-DC system initials.

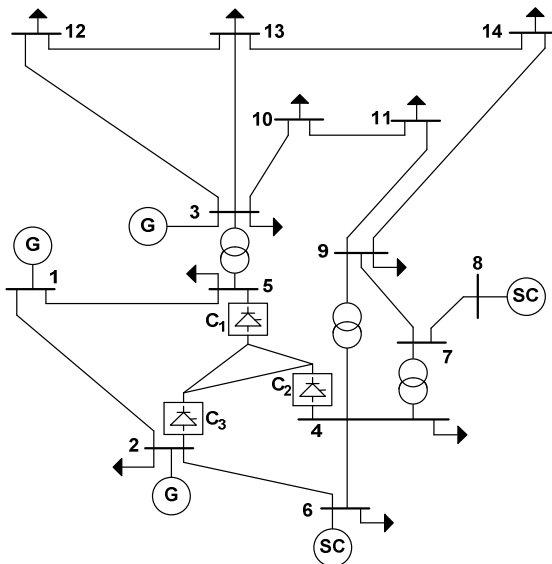


Figure 7. The modified IEEE 14-bus AC-DC test system

GA reaches to global optimum at about approximately 60<sup>th</sup> iteration for the best trial. For GA: population size is selected as 22, crossover rate is selected as 0.5 and mutation rate is selected as 0.1. The selected parameter values used for GA are determined with enough trials. The upper values of the used ones do not change the global optimum point for GA. The case of using higher sizes than the determined values given above decreases the number of iteration where the global optimum point is achieved. But this situation increases the optimization time of reaching the global optimum point. The penalty coefficient values  $c_i$  that are used in (41) are determined after several trials. For the 50 optimization trials, the worst and the best total active power loss values for GA are 0.107 p.u. and 0.105 p.u., respectively. Error deviation for GA is 1.87%. It is proved from the test results that all of the control and the state variables are kept in the determined limit values at the end of the optimization.

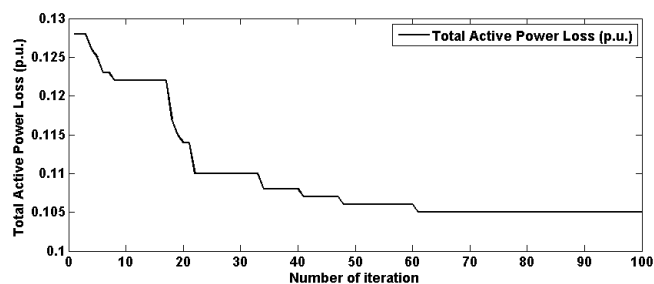


Figure 8. Variation of total active power loss against iteration for the proposed approach ( $P_{base} = 100MW$ )

The presented approach can achieve better global optimum point for providing minimum active power loss than the compared traditional technique SDA [23] as seen in Table 1.

Table 1. Comparison of the results for the test system

	GA	SDA [23]
Total Active Power Loss (p.u.)	0.105	0.131

## 6. CONCLUSION

In the presented paper, a novel approach is proposed for the optimal reactive power flow of active power loss minimization in multi-terminal HVDC systems. GA is used for the first time in multi-terminal HVDC system for optimal reactive power flow solution in this study. As the sequential technique is used in the presented AC-DC power flow study, any kind of AC and DC power flow techniques can be performed in the proposed approach without need of any change in the optimization algorithm. Active power values of the DC converters are selected as control variables for optimization in the whole DC system in the study unlike the similar studies in the literature. Thus, both the best suitable active power values of the converters ( $p_{di}^{min} \leq p_{di} \leq p_{di}^{max}$ ) and the best suitable converter operation mode are determined for the defined system conditions. Thus, efficiency of the achieving minimum active power loss is enhanced. The obtained results from the optimization study have shown that the presented approach is accurate and efficient for reaching the global optimum point than the traditional numerical optimization methods without dropping to local minimum points. The proposed approach also meets the system

constraints for security and healthy system operation.

## REFERENCES

- [1] H. Wei, C. Lin and Y. Wang, "The optimal reactive power flow model in mixed polar form based on transformer dummy nodes", *IEEJ Transactions on Electrical and Electronic Engineering*, vol. 13, no. 3, pp. 411–416, 2018.
- [2] Y.A. Mobarak, "Modified load flow analysis for integrated ac/dc power systems", *12th Int. Middle East Power Syst. Conf. MEPCON*, pp. 481–484, 2008.
- [3] J.R. De Silva and C.P. Arnold, "A simple improvement to sequential ac/dc power flow algorithms", *International Journal of Electrical Power & Energy Systems*, vol. 12, no. 3, pp. 219–221, 1990.
- [4] U. Arifoglu, "Load flow based on newton's method using norton equivalent circuit for ac-dc multiterminal systems", *European Transactions on Electrical Power*, vol. 9, no. 3, pp. 167–174, 1999.
- [5] D. Thukaram and G. Yesuratnam, "Optimal reactive power dispatch in a large power system with ac-dc and FACTS controllers", *IET Generation Transmission & Distribution*, vol. 2, no. 1, pp. 71–81, 2008.
- [6] D. Thukaram, G. Yesuratnam, and C. Vyjayanthi, "Optimal reactive power dispatch based on voltage stability criteria in a large power system with ac/dc and FACTS devices", *IEEE Int. Conf. Power Electro. Drives Energy Syst. PEDES*, 2006.
- [7] J. Yu, W. Yan, W. Li and L. Wen, "Quadratic models of ac-dc power flow and optimal reactive power flow with HVDC and UPFC controls", *Electric Power Systems Research*, vol. 78, no. 3, pp. 302–310, 2008.
- [8] J. Yu, W. Yan, W. Li, C.Y. Chung and K.P. Wong, "An unfixed piecewise-optimal reactive power-flow model and its algorithm for ac-dc systems", *IEEE Transactions on*

- Power Systems*, vol. 23, no. 1, pp. 170–176, 2008.
- [9] U. De Martinis, F. Gagliardi, A. Losi, V. Mangoni and F. Rossi, “Optimal load flow for electrical power systems with multiterminal HVDC links”, *IEE Proceedings Generation Transmission and Distribution*, vol. 137, no. 2, pp. 139–145, 1990.
- [10] C.N. Lu, S.S. Chen and C.M. Ong, “The incorporation of HVDC equations in optimal power flow methods using sequential quadratic programming techniques”, *IEEE Transactions on Power Systems*, vol. 3, no. 3, pp. 1005–1011, 1988.
- [11] H. Ambriz-Perez, E. Acha and C.R. Fuerte-Esquivel, “High voltage direct current modelling in optimal power flows”, *International Journal of Electrical Power & Energy Systems*, vol. 30, no. 3, pp. 157–168, 2008.
- [12] U. Arifoglu and N. Tarkan, “New sequential ac-dc load-flow approach utilizing optimization techniques”, *European Transactions on Electrical Power*, vol. 9, no. 2, pp. 93–100, 1999.
- [13] K. Ayan and U. Kilic, “Artificial bee colony algorithm solution for optimal reactive power flow”, *Applied Soft Computing*, vol. 12, no. 5, pp. 1477–1482, 2012.
- [14] Y. Kabalci, “An improved approximation for the Nakagami-m inverse CDF using artificial bee colony optimization”, *Wireless Networks*, vol. 24, no. 2, pp. 663–669, 2018.
- [15] L. Wang and L. Li, “A coevolutionary differential evolution with harmony search for reliability-redundancy optimization”, *Expert Systems with Applications*, vol. 39, no. 5, pp. 5271–5278, 2012.
- [16] M. Gomez-Gonzalez, A. Lopez and F. Jurado, “Optimization of distributed generation systems using a new discrete PSO and OPF”, *Electric Power Systems Research*, vol. 84, no. 1, pp. 174–180, 2012.
- [17] O.P. Verma, P. Kumar, M. Hanmandlu and S. Chhabra, “High dynamic range optimal fuzzy color image enhancement using artificial ant colony system”, *Applied Soft Computing*, vol. 12, no. 1, pp. 394–404, 2012.
- [18] U. Guvenc, B.E. Altun and S. Duman, “Optimal power flow using genetic algorithm based on similarity”, *Energy Education Science and Technology Part A: Energy Science and Research*, vol. 29, no. 1, pp. 1–10, 2012.
- [19] M.S. Kumari and S. Maheswarapu, “Enhanced genetic algorithm based computation technique for multi-objective optimal power flow solution”, *International Journal of Electrical Power & Energy Systems*, vol. 32, no. 6, pp. 736–742, 2010.
- [20] F. Yalcin and U. Arifoglu, “Inserting the tap values of the tap changer transformers into the Jacobian matrix as control variables”, *Sakarya University Journal of Science*, vol. 17, no. 3, pp. 337–348, 2013.
- [21] J.H. Holland, *Adaptation in Natural and Artificial Systems*, Michigan: University of Michigan Press, 1975.
- [22] MATLAB Optimization Toolbox 5 User’s Guide (2012) The Math Works, Inc.
- [23] Ugur Arifoglu, “Optimal power flow using sequential power flow approach for an ac-dc power system”, Ph. D. thesis, Istanbul Technical University, Istanbul, 1993.